



POLITECNICO
MILANO 1863

DIPARTIMENTO DI MECCANICA



Thin wall geometrical quality improvement in Micromilling

ANNONI, MASSIMILIANO PIETRO GIOVANNI; REBAIOLI, LARA;
SEMERARO, QUIRICO

This is a post-peer-review, pre-copyedit version of an article published in International Journal of Advanced Manufacturing Technology. The final authenticated version is available online at: <http://dx.doi.org/10.1007/s00170-015-6862-3>

This content is provided under [CC BY-NC-ND 4.0](https://creativecommons.org/licenses/by-nc-nd/4.0/) license



Thin wall geometrical quality improvement in micromilling

M. Annoni, L. Rebaioli, Q. Semeraro

Dipartimento di Meccanica

Politecnico di Milano

Milano, Italy

ABSTRACT

Micromilling is one of the most versatile tooling processes that is able to effectively manufacture three-dimensional complex features on molds and dies achieving a good accuracy performance. Typical and challenging features for these microcomponents are high aspect ratio thin walls. The present study focuses on 0.4 % carbon steel (C40) thin wall micromilling and evaluates two approaches for the thin wall geometrical quality improvement: a direct approach and a force-based approach. A suitable experimental campaign has been designed in order to statistically analyse the cutting force responses and a proper technique (ANalysis of COVAriance) has been applied to remove the tool wear effect. The feasibility of a general approach able to meet tolerances by controlling forces has been demonstrated by coupling the relationship established between cutting forces and workpiece geometrical quality with the effect of some nominal workpiece characteristics / process parameters on wall quality and cutting forces.

KEYWORDS

micromilling, thin wall, wall thickness, flatness deviation, cutting forces, ANCOVA

1. INTRODUCTION

Micromilling is a fundamental process for producing 3D complex microparts such as tools for other processes (molds for micromolding, microforming and micro-extrusion). Features characterized by a high aspect ratio (AR) i.e. ratio between height and thickness, such as walls, pins, etc. are common features in molds [1-2]. The present study focuses on thin walls since these features represent a typical challenge in micromilling and often require very tight tolerances (e.g. in microfluidic applications [3]). Thin wall micromilling is critical since cutting forces produce wall bending or vibrations that reduce the feature final quality in terms of flatness and straightness. Macro scale strategies for

thin wall machining are a good starting point, but they must be redesigned in case of micromilling operations in order to cope with the low stiffness of features and tools.

Figure 1 depicts two different approaches that can be followed in order to predict the workpiece quality and points out some representing papers where they were described and used. The direct approach (“1”, green arrow) [4-7] directly predicts the feature geometrical quality from the nominal workpiece characteristics and the process parameters combination, while the force-based approach (“2” and “3”, red arrows) [6, 8-15] predicts the workpiece quality basing on the cutting forces effects during micromilling operations. According to this approach, forces are predicted from the process parameters combination. The force-based approach attempts to open and explain the process parameters relationship with the workpiece quality introducing physical quantities, such as forces, suitable for monitoring and controlling purposes.

A possible real-time control system could base its decisions on forces, which are easily measurable in-process; the control system could try, for example, to meet tolerances by obtaining the designed force values acting on process parameters. Meeting tolerances by simply controlling the process parameters values, according to the direct approach, is not enough in micromilling since tool and feature bending cannot be evaluated without considering forces. Moreover, this approach cannot be implemented in a real-time control system because the workpiece quality is difficult to measure in-process.

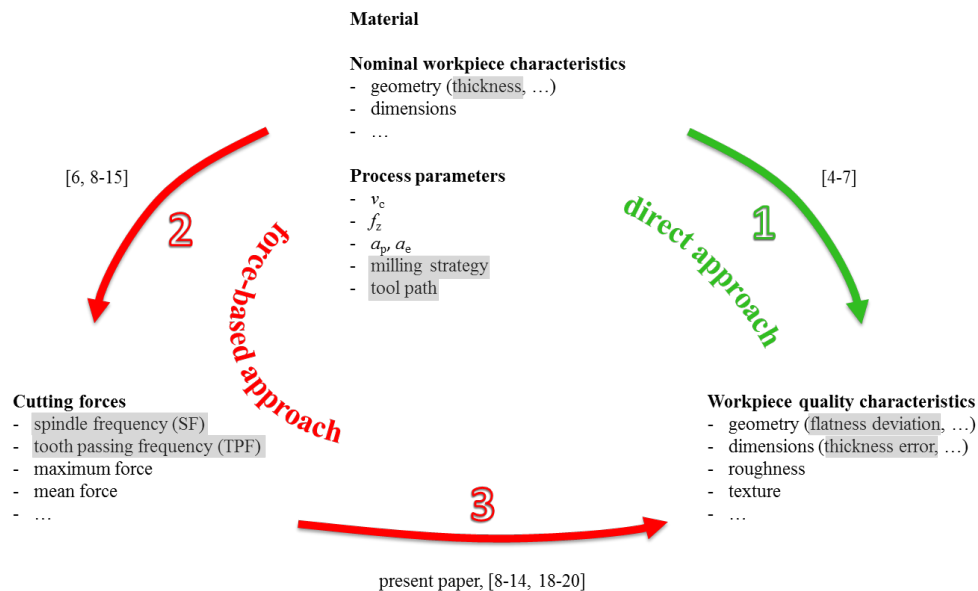


Figure 1. Different approaches for predicting the workpiece quality (grey: quantities considered in the present study).

In a previous study [4], the same authors of the present paper carried out thin wall milling with a maximum AR of

300 (3 mm x 10 μ m) on 0.4 % carbon steel (C40). In this research, the authors systematically investigated and identified a direct relationship between nominal workpiece characteristics / process parameters and workpiece quality in case of thin wall micromilling (“1”, green arrow in Figure 1). A following study by the same authors [15] pointed out the nominal workpiece characteristics / process parameters effect on cutting forces (“2”, red arrow in Figure 1) and defined some preliminary criteria for selecting the correct parameters combination to obtain the desired cutting forces. This work represented a first step towards a force-based quality monitoring and control system and its first results allowed to draw some qualitative considerations on the relationship between cutting forces and thin wall quality (“3”, red arrow in Figure 1).

The present paper aims at quantitatively studying the relationship between cutting forces and workpiece quality (“3”, red arrow in Figure 1) in order to demonstrate the feasibility of the force-based approach.

2. STATE OF THE ART

Compensation techniques for geometric and thermal errors have successfully improved machine tool accuracy, but cutting force-induced errors are still often neglected since cutting forces are low and the workpiece deflections could be ignored in finishing operations [16-17]. However, hardened steel machining is now widely performed, hence, cutting forces could be very large compared to the workpiece stiffness, especially in case of high aspect ratio features, and the resulting errors should be taken into account since they could represent the main error sources. In this regard, Wang et al. [18] and Gao et al. [19] developed real-time compensation strategies for force-induced errors, respectively in multi-axis machining and in precision boring of high aspect ratio holes. Both methods are based on measured forces and their relationship with measured errors. On the other hand, Law et al. [8] developed a compensation methodology for pocket end milling that integrates a cutting force model and a discrete deflection model.

Regarding thin walls, the features on which the present paper focuses, Ratchev et al. [9-13] proposed an error compensation strategy based on an analytical force model integrated with a finite element model for the workpiece deflection prediction during machining. Also Chen et al. [20] developed an error compensation approach for multilayer milling of thin-walled parts which considers only the workpiece bending due to cutting forces. On the other hand, the error control strategy by Wan et al. [14] relies on a mechanistic model for predicting the cutting forces, a finite element method for estimating the workpiece deflection and also a cantilever beam model for evaluating the tool deflection.

Several studies concerning thin wall milling in the microscale can be found in literature [5-7, 21-25]. Only few of them (e.g. [5-7]) focus on finding the best machining conditions to obtain good quality walls, while most of them [21-25] simply show the capability to machine very challenging high aspect ratio walls. None of these studies deals

with cutting force-induced errors compensation.

In their study, Popov et al. [5] machined high aspect ratio structures with $650\ \mu\text{m} \times 20\ \mu\text{m}$ dimensions ($AR = 32.5$) by applying special micromilling tool paths in order to avoid thin wall bending due to cutting forces. Nevertheless, cutting forces were not measured during tool path experimental validation and only a qualitative approach was applied to study the wall deformation and thickness error.

Li et al. [6] obtained $800\ \mu\text{m}$ deep and $15\ \mu\text{m}$ thick thin walls ($AR = 54$) on Böhler M261 mold steel. Their work was devoted to study the challenges in micromilling thin walls with high aspect ratio and took into account the effect on the wall surface of different cutting parameters, milling strategies and tool paths. The obtained workpiece quality was evaluated only in a qualitative way using SEM images. Finite elements analysis was used to predict the tool path effect on the machined thin wall flatness. Eventually, the authors also investigated the relationship between machining parameters (namely, feed per tooth, depth of cut and width of cut) and cutting forces by means of an analytical cutting force prediction model.

In their work, Llanos et al. [7] focused on studying the effect on thin wall roughness and quality of different cutting parameters (namely, spindle speed, feed rate, axial and radial depth of cut), nominal wall thicknesses, milling strategies and tool paths; cutting forces were not taken into account. The obtained workpiece roughness was measured by an optical profiler while geometrical quality was evaluated only in a qualitative way basing on SEM images. In their study, these authors obtained $750\ \mu\text{m}$ deep and $50\ \mu\text{m}$ thick thin walls ($AR = 15$) and $1.5\ \text{mm}$ deep and $25, 50, 75\ \mu\text{m}$ thick thin walls ($AR = 60, 30, 20$) on CuZn36Pb3 brass and 6061-T4 aluminum.

Friedrich et al. [21] used PMMA (polymethyl methacrylate) as working material and they obtained thin walls characterized by an aspect ratio almost equal to 8 (depth $62\ \mu\text{m}$; thickness $8\ \mu\text{m}$) by milling spiral trenches thanks to a specially designed high-precision machine. The authors did not point out the relationship between process parameters and workpiece quality, but they just concentrated on obtaining high aspect ratio walls.

The study of Bang et al. [22] describes the design and testing of a selfmade PC-based 5-axis micromilling machine. To validate their design, the authors machined several features such as thin walls, high aspect ratio pins, micro impellers and micro blades. As concerning thin walls, they succeeded in milling $650\ \mu\text{m} \times 25\ \mu\text{m}$ walls (corresponding to an aspect ratio of 26) on brass; they divided the wall height into several layers of a few micrometres, which were sequentially machined. However, no different process parameter sets were investigated, no workpiece quality measurements were performed and cutting forces were not considered.

In their paper, Gietzelt et al. [23] showed two examples of high aspect ratio microstructures machined on ceramic materials: $200\ \mu\text{m}$ thick walls on glassy ceramic and walls with an aspect ratio of 10 ($2\ \text{mm}$ deep and $200\ \mu\text{m}$ thick) on presintered zirconia. The authors do not report neither workpiece quality nor cutting force measurements.

Okazaki et al. [24-25] built desktop milling machines with ultra-high spindle speeds and tested them by milling very challenging features; they selected a high strength aluminium alloy as target material (A7075-T651) and succeeded in machining 2 mm x 80 μ m straight walls (AR = 25) and 1.5 mm x 30 μ m annular walls (AR = 50) by a 0.5 mm end mill. Their work was only devoted to design and validate their selfmade machines: they just concentrated on successfully obtaining high aspect ratio walls and did not test different machining strategies.

In conclusion, specific literature provides a basic knowledge which helps to find out the process parameters and outcomes of interest in thin wall micromilling. However, no systematic approaches exist dealing with the relationship between nominal workpiece characteristics / process parameters, cutting forces and workpiece quality, which is the target of the present study.

3. OBJECTIVES AND DEFINITIONS

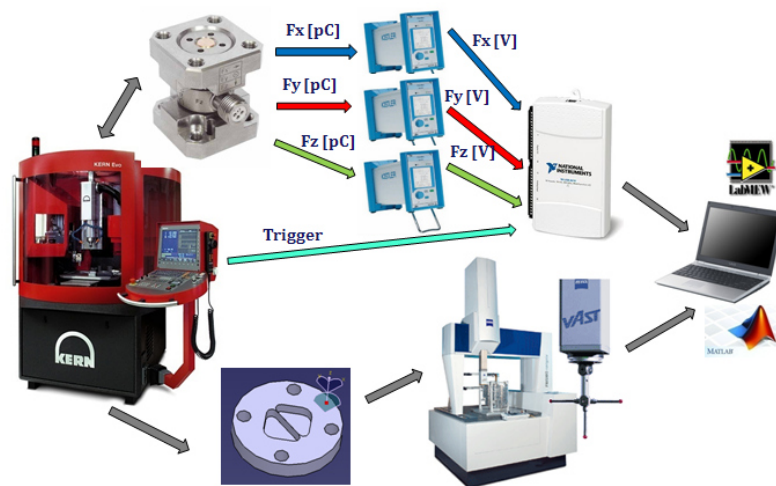


Figure 2. Measurement chains: cutting forces (top) and workpiece quality (bottom).

The present study started from results on the effect of some nominal workpiece characteristics / process parameters (wall thickness, milling strategy and tool path) on workpiece quality (thickness error and flatness deviation [4]) and on cutting forces [15] in high aspect ratio wall micromilling, with the aim of objectively evaluating the relationships between cutting forces and wall quality.

The experimental responses can be divided in two families: workpiece quality and cutting forces, hence two measurement chains are needed (Figure 2).

This section describes quantities, procedures and conventions applied in this study to achieve the defined objectives.

3.1. Workpiece geometry, machining center and working operation definition

A proper workpiece (Figure 3) has been designed in order to allow both cutting force acquisition during thin wall machining (Figure 4) and wall deformation measurements. The workpiece has two triangular slots that define the thin wall, whose height and length are respectively 3 mm and 10 mm. The workpiece has an outer diameter of 30 mm and is made up of 0.4 % carbon steel (C40).

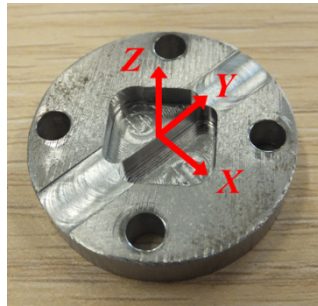


Figure 3. Workpiece and machine reference system.

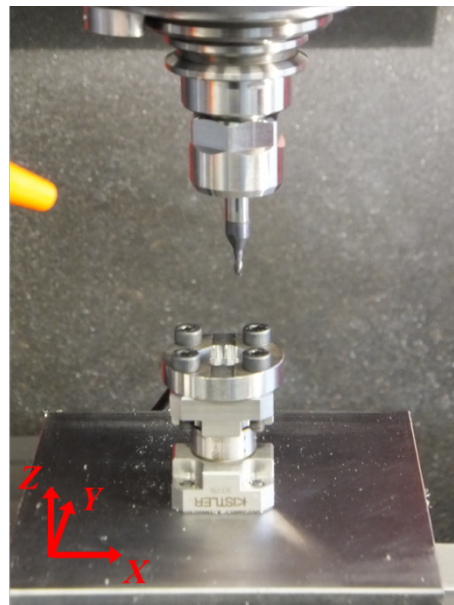


Figure 4. Workpiece mounted on the Kistler 9317B load cell.

The Kern EVO ultra precision 5-axis machining center available at the “MI_crolab” of Dipartimento di Meccanica of Politecnico di Milano (nominal positioning tolerance = $\pm 1 \mu\text{m}$, precision on the workpiece = $\pm 2 \mu\text{m}$) has been used

to perform thin wall machining.

Table 1. Constant cutting parameters for thin wall milling.

| | <i>cutting speed</i> | <i>feed</i> | <i>axial depth</i> | <i>radial depth</i> |
|-----------|----------------------|-------------|--------------------|---------------------|
| | V_c [26] | f_z [27] | a_p [27] | a_e [27] |
| | m/min | mm/tooth | mm | mm |
| roughing | 151 | 0.02 | 0.5 | 0.3 |
| finishing | 126 | 0.02 | 0.5 | 0.2 |

The present study has focused on the final thin wall quality, hence only the finishing operation has been considered in the experiments while the roughing operation has been performed before each run using different cutting parameters. Cutting parameters reported in Table 1 have been kept constant in every test.

Thin wall machining have been carried out by means of hard metal end-mills. Mill brand and characteristics have been: Sandvik Coromill Plura R216.12-02030-BS30P; D_c (cutting diameter) = 2 mm; z (teeth number) = 2, θ_h (helix angle) = 30° , γ_f (radial rake angle) = 10.5° .

Cutting parameters used for wall finishing (reported in Table 1) have been centered in the selected mill operating window, which was determined in a preliminary experimental campaign based on the mill manufacturer instructions [28].

3.2. Experimental design

A proper factorial experimental design, summarized in Table 2, has been studied to point out the effects of the selected nominal workpiece characteristics / process parameters (wall thickness, milling strategy and tool path) on wall quality and cutting forces.

Each experimental condition has been replicated twice, hence the whole experimental design has consisted of 32 runs, which have been completely randomized.

Table 2. Experimental design summary.

| <i>Factor</i> | <i>Symbol</i> | <i>Levels</i> |
|---------------|---------------|---------------------------------|
| Thickness | TH | 10, 30, 50 and 70 μm |
| Strategy | S | Up-milling, Down-milling |
| Tool path | TP | Waterline, Step Support |

Section 3.3 describes the nominal workpiece characteristics / process parameters that are considered as experimental factors in the present study. The experimental responses can be divided in two families, workpiece quality characteristics and cutting forces, that are discussed respectively in Section 3.4 and 3.5.

3.3. Experimental factors

The Thickness factor, representing the nominal wall thickness, has been varied on four levels (10, 30, 50 and 70 μm) while two levels have been considered for the Strategy factor (“Up-milling” and “Down-milling”) and for the Tool path factor (“Waterline” and “Step Support”, Figure 5).

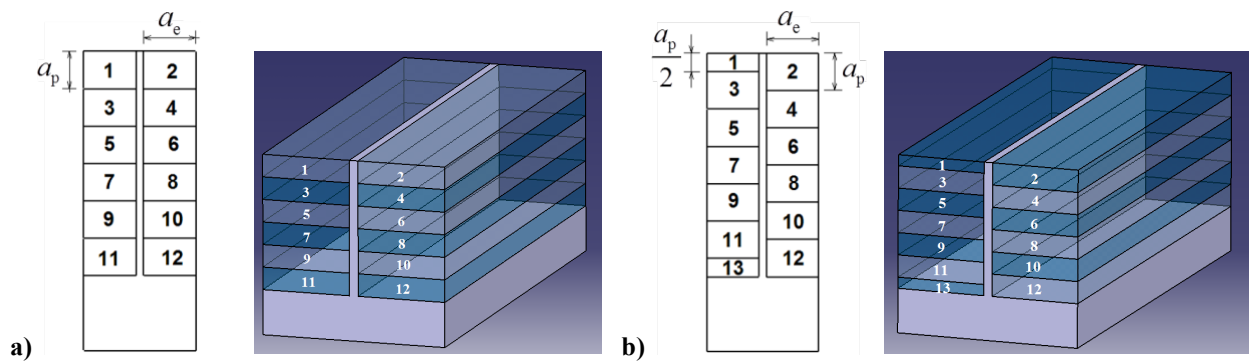


Figure 5. Tool paths for thin wall machining: a) Waterline and b) Step Support tool paths (dimensions not in scale).

Figure 5 depicts the studied tool paths (the same tool paths were evaluated by Li et al. [6] and Llanos et al. [7], which also considered a ramp tool path). Steps have been machined alternatively on the left and right sides of the wall in both tool paths, but all steps have had the same axial depth in case of Waterline milling operations (Figure 5a) while the first step has been machined at half axial depth in the Step Support tool path (Figure 5b) in order to partially support

the wall when milling the other side.

3.4. Geometrical measurements

Tool radius. A proper statistical technique (ANalysis of COVariance) has been used in order to take into account the tool wear effect on wall geometrical quality and cutting forces. Tool wear is expected to act as a nuisance factor, therefore, in order to remove its effect by means of ANCOVA, the cumulative tool radius variation (ΔR_{cum}) has been measured. Tool radius variation has been obtained as the difference between the tool radius measured before and after each wall finishing operation. The Blum Micro Compact NT laser presetting system (accuracy: 1 μm) available on the Kern EVO machining center has been used to measure the tool radius. ΔR_{cum} is the sum of the tool radius variations till the current experimental run and has been considered as covariate in the statistical analysis (Section 5.1 and 5.2).

Workpiece quality. Thin wall geometrical quality has been evaluated in terms of two geometrical characteristics: the total flatness deviation and the average thickness error.

Wall flatness and thickness have been measured using a Zeiss Prismo 5 HTG VAST coordinate measuring machine (maximum single-stylus form error $P_{FTU,MPE} = 2 \mu\text{m}$ [29]), equipped with a 1 mm diameter touch probe; such a CMM was selected since different measuring instruments would not have been able to acquire the whole wall profile in the same setup.

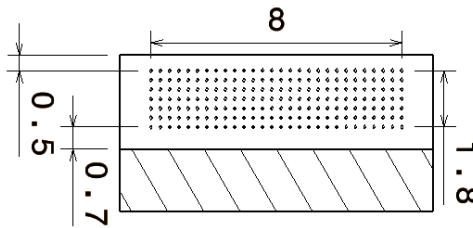


Figure 6. Measurement points grid on one side of the wall (dimensions in millimeters).

Walls have been sampled on a regular square grid with a density of 1 point every 0.3^2 mm^2 ; hence 196 points (28 x 7, Figure 6) have been acquired on both sides of the wall. The CMM elastic part deformation compensation algorithm has been applied to measurements, hence the wall elastic deformation has been compensated by sampling each point with different loads (50 and 100 mN) and then estimating the correct measurement result; the application of the load compensation with different loads has always lead to the same results, thus ensuring measurement trueness. Figure 7 shows the CMM measurement results for a couple of specimens.

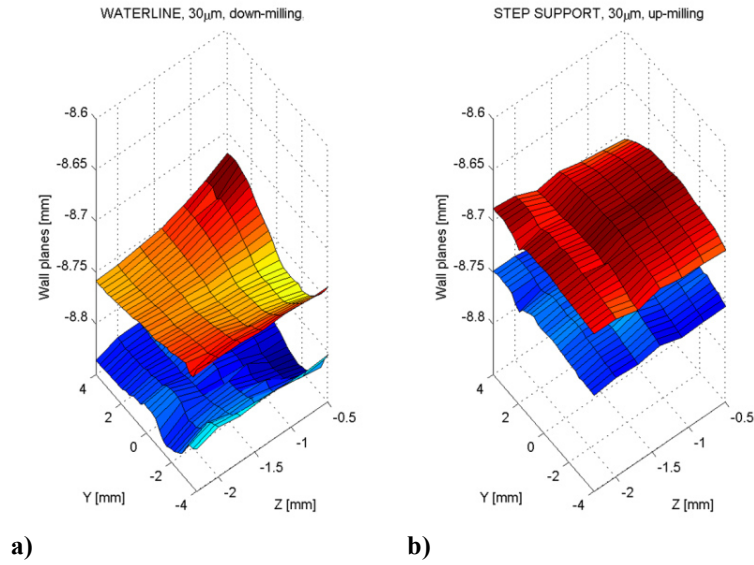


Figure 7. Wall left and right surfaces from CMM measured points: a) Waterline, 30 μm nominal thickness, Down-milling, b) Step Support, 30 μm nominal thickness, Up-milling.

The average thickness absolute error has been evaluated for each run considering the nominal thickness according to the following equation:

$$err = T_{\text{mean,eff}} - T_{\text{nom}} \quad (1)$$

where $T_{\text{mean,eff}}$ is the effective mean thickness calculated by the CMM [30] and T_{nom} is the nominal thickness.

The total flatness deviation has been measured according to the minimum zone principle [31] for both the wall surfaces (Figure 7). A paired t-test was applied to determine if the observed flatness errors of the left and right surfaces were statistically different. Test p-value was equal to 0.107, hence it is possible to presume that both sides of each wall present a non-statistically different flatness deviation. Therefore, only left wall surface total flatness deviation has been taken as wall geometrical quality response together with the average thickness error.

3.5. Force measurements

Cutting force signals have been measured by means of a Kistler 9317B triaxial piezoelectric load cell (measuring range: $F_x, F_y = \pm 1000 \text{ N}$, $F_z = \pm 2000 \text{ N}$; linearity error $\leq 0.5\%$ FSO, Full Scale Output) amplified by three Kistler 5015A charge amplifiers and acquired by a National Instrument USB 6210 board at a 40000 Hz sampling frequency. A

low-pass filter at 20000 Hz has been applied directly on the charge amplifiers in order to avoid aliasing and a Hanning window has been used to reduce leakage. The acquisition length has been 0.75 s for each milling step. Only forces perpendicular to the wall, i.e. in X direction (Figure 3), have been considered in the following, since they reasonably are the main responsible for wall bending.

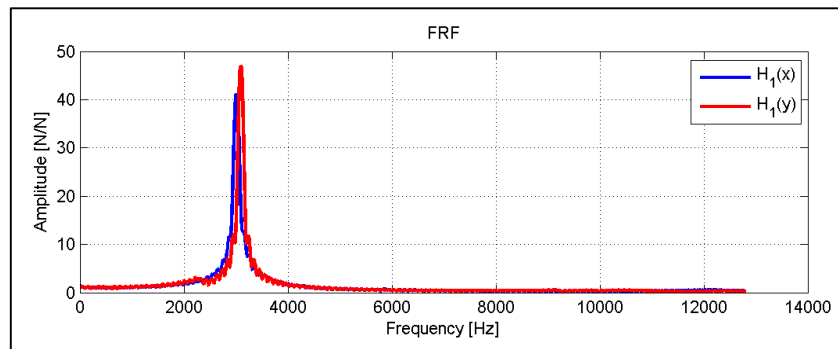


Figure 8. Frequency Response Function (FRF) resulting from an impact test on the fixturing and force measurement system [F_x = blue, F_y = red].

Cutting force measurements are affected by vibrations due to the low resonance frequency of the fixturing and force measurement system, which is approximately 3000 Hz in both X and Y directions, as pointed out in Figure 8. The FRF depicted in Figure 8 results from an impact test on the fixturing and force measurement system, therefore it has a “N/N” unit since it represents the response function between the force measured by the load cell (output) and the force applied by the dynamometric hammer (input). This FRF is similar to the so-called “receptance”, whose output is the displacement, because a displacement causes an electric charge variation which in turn changes the force measured by the load cell.

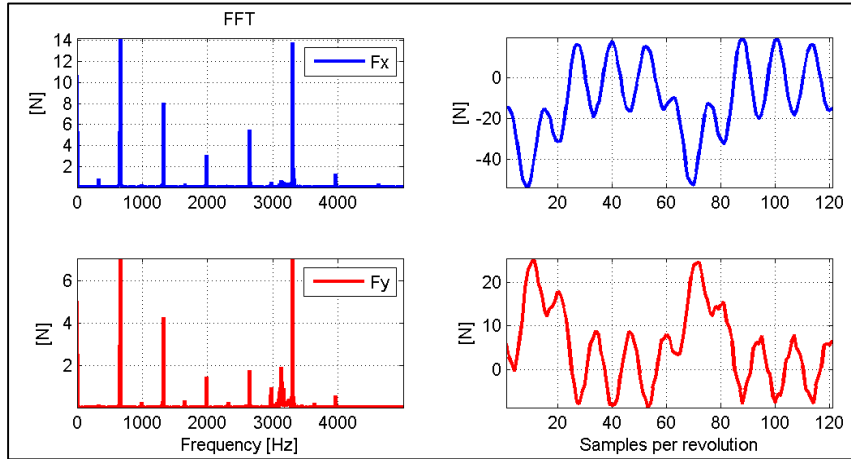


Figure 9. Fast Fourier Transform (FFT) (left) and time domain plot detail (right) of a cutting force acquisition example

$[V_c = 126 \text{ m/min}, f_z = 0.02 \text{ mm/tooth}, a_p = 0.5 \text{ mm}, a_e = 0.2 \text{ mm}, \text{wall thickness} = 200 \mu\text{m}] (F_x = \text{blue}, F_y = \text{red}).$

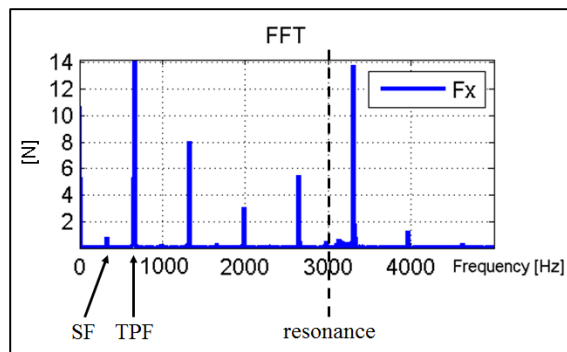


Figure 10. Spindle Frequency (SF) and Tooth Passing Frequency (TPF) harmonic components [see Figure 9 caption for the applied working parameters].

Vibration effects are evident in both time and frequency domains (Figure 9). The force harmonic components close to the system resonance frequency excite the system, hence their amplitude is amplified.

When milling a thin wall, the system modal parameters (namely mass, stiffness and damping) vary with the milling steps because of the material removal. The variation of these properties directly affects the resonance frequency, which is consequently not constant along the steps: for example, peaks of Figure 8 are likely to move to the right during milling operations due to the workpiece mass reduction. Predicting the modal parameters and resonance frequency variations is quite complicated and results are not general since they depend on workpiece geometry, tool path and cutting parameters.

For these reasons, it has been decided to limit the analysis to the first signal harmonic components, i.e. the Spindle Frequency (SF, which is equal to $n/60$, where n is the spindle speed expressed in rpm) and the Tooth Passing Frequency (TPF, which is equal to $SF \cdot z$, where z is the teeth number), which are sufficiently informative and not affected by resonance. Since the cutting speed has been constant for all the experiments, SF and TPF have been always the same (respectively, 333 Hz and 666 Hz) and far from the system resonance frequency (Figure 10).

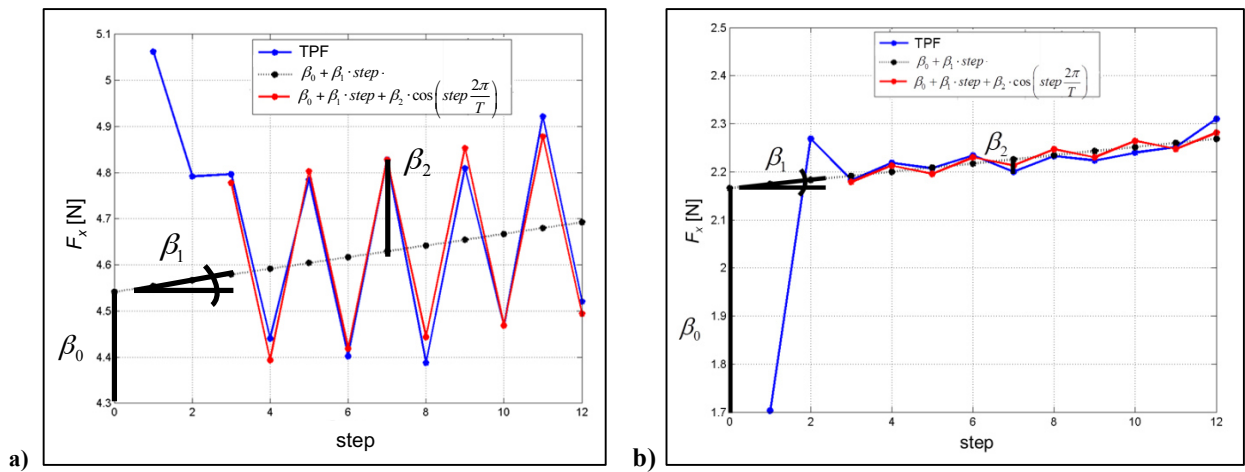


Figure 11. TPF amplitude against milling steps [10 μm thickness, down-milling strategy and a) Waterline tool path, b) Step Support tool path] (Y axis has been enlarged to highlight TPF behavior).

The SF and TPF harmonic component amplitude (named SF and TPF in the following for the sake of simplicity) have been plotted against the finishing operation steps for each run of the experimental plan, where one run corresponds to one wall finishing operation carried out with a certain combination of wall thickness, milling strategy and tool path. For example, Figure 11a represents the TPF profile in a test with 10 μm wall thickness, down-milling strategy and Waterline tool path. It can be noticed that the TPF mean value increases with the steps probably because the tool friction on the machined wall gets higher as the mill moves down. It can also be observed that a TPF reduction takes place at even steps due to the wall bending under the cutting force when not supported on the other side (Waterline tool path, Figure 5a); this effect makes actual radial depth of cut smaller than its nominal value and reduces forces. As can be noticed in Figure 11b, the TPF value variations are smaller when milling with the Step Support tool path (Figure 5b) and the cutting force action is counteracted by the material left on the opposite wall side.

The following regression model has been applied on each SF and TPF profile in order to fit experimental data:

$$Y = \beta_0 + \beta_1 \cdot step + \beta_2 \cdot \cos\left(step \frac{2\pi}{T}\right) \quad (2)$$

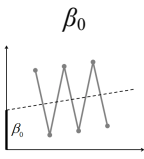
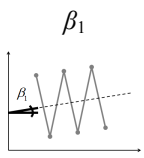
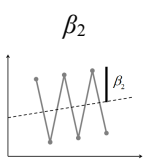
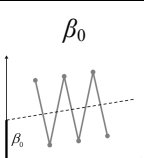
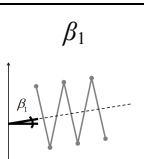
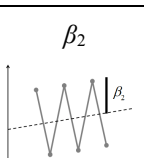
where *step* is the milling step number.

The regression model coefficients represent the intercept β_0 , the slope β_1 and the oscillation amplitude β_2 of the harmonic components when plotted against milling steps (Figure 11). The three coefficient estimates $\hat{\beta}_0$, $\hat{\beta}_1$ and $\hat{\beta}_2$ have been calculated at each run and have been used as experimental response variables. For the sake of simplicity, the estimates will be named β_0 , β_1 and β_2 in the following.

Each experimental run has produced six force responses, three for SF and three for TPF, in addition to the two wall geometry responses (total flatness deviation and average thickness error).

4. EXPERIMENTAL RESULTS

Table 3. ANCOVA p-values (dark grey = significant factor, grey = nearly significant factor, $\alpha = 1\%$).

| | | Factors | | | | | | | | Estimated standard deviation (σ) | | |
|-----------|----------------|-------------------------------|---|--------------|----------------|--------------|--------------|--------------|--------------|---|--------------|---------|
| | | ΔR_{cum} | Thickness (TH) | Strategy (S) | Tool path (TP) | TH*S | TH*TP | S*TP | TH*S*TP | | | |
| Responses | Wall quality | Flatness deviation | 0.018 | 0.000 | 0.001 | 0.739 | 0.039 | 0.142 | 0.023 | 0.040 | 0.01025 | |
| | | Thickness error | 0.014 | 0.000 | 0.000 | 0.096 | 0.000 | 0.094 | 0.517 | 0.088 | 0.00322 | |
| | Cutting forces | Spindle Frequency (SF) |  | 0.000 | 0.825 | 0.000 | 0.254 | 0.657 | 0.614 | 0.116 | 0.074 | 0.25944 |
| | | |  | 0.000 | 0.488 | 0.000 | 0.676 | 0.300 | 0.514 | 0.005 | 0.116 | 0.00935 |
| | | |  | 0.002 | 0.663 | 0.003 | 0.000 | 0.652 | 0.203 | 0.032 | 0.357 | 0.03114 |
| | | Tooth Passing Frequency (TPF) |  | 0.027 | 0.111 | 0.000 | 0.113 | 0.131 | 0.062 | 0.341 | 0.010 | 0.28064 |
| | | |  | 0.001 | 0.723 | 0.047 | 0.499 | 0.345 | 0.159 | 0.050 | 0.013 | 0.00664 |
| | | |  | 0.275 | 0.000 | 0.001 | 0.000 | 0.001 | 0.000 | 0.006 | 0.015 | 0.01996 |

4.1. Relationship between nominal workpiece characteristics / process parameters and workpiece quality

A three factors (Thickness, Strategy and Tool path) complete model plus the covariate ΔR_{cum} (cumulative tool radius variation) has been analyzed in order to study the relationship between the nominal workpiece characteristics / process parameters and the workpiece geometrical quality (“1”, green arrow in Figure 1).

The results of ANCOVA on wall quality responses are summarized in Table 3 while Figure 12, 13 and 14 detail the results related to the average thickness error and the total flatness deviation for each factor.

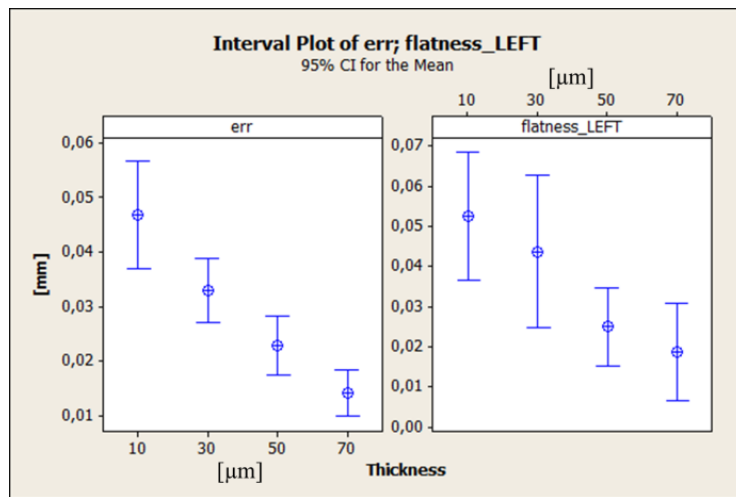


Figure 12. Interval value plots of wall quality responses against Thickness factor.

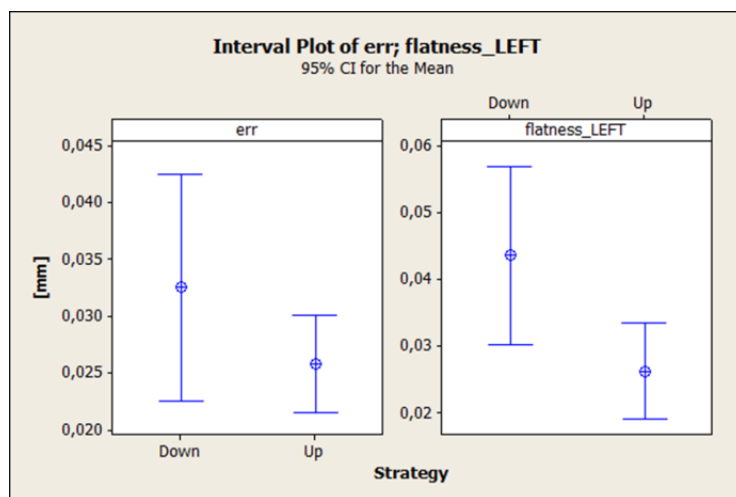


Figure 13. Interval value plots of wall quality responses against Strategy factor.

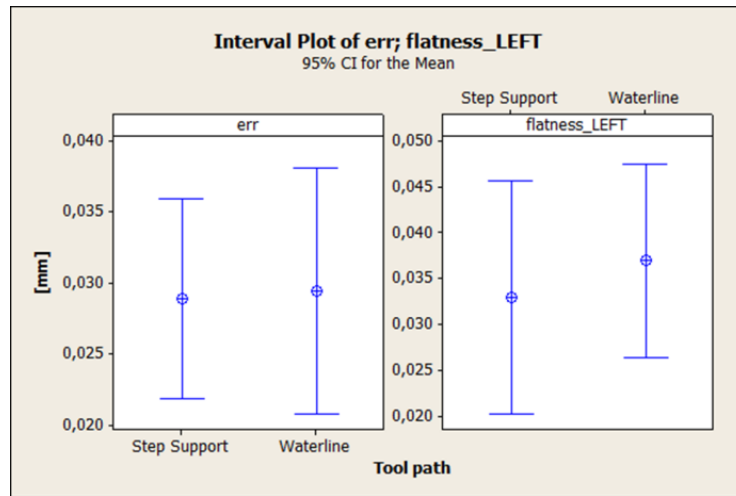


Figure 14. Interval value plots of wall quality responses against Tool path factor.

As regarding the relationship between the process parameters and, respectively, the workpiece geometrical quality (“1”, green arrow in Figure 1) the covariate significance (Table 3) means that the tool edge becomes dull as the tool wear increases; this way, the accuracy on the finished wall decreases in terms of mean thickness.

The flatness deviation and the average thickness absolute error show higher values when the nominal thickness reaches the lowest values, i.e. 10 and 30 μm (Figure 12), since the wall becomes more flexible (e.g. this means that the actual mean thickness is around 57 μm for a nominal thickness of 10 μm and around 84 μm for a nominal thickness of 70 μm).

The last factor which affects the geometrical responses is the strategy (Table 3): Down-milling is more critical because when the wall (and/or the tool) bends, the actual depth of cut value is reduced more than in the Up-milling case. Therefore, when the wall is down-milled in the finishing phase, both average wall thickness and flatness deviation show higher values (Figure 13), thus leading to errors in terms of geometrical accuracy (e.g. average thickness absolute error and flatness deviation go, respectively, from 34.5 and 43.5 μm for Down-milling to 26.2 and 26.8 μm for Up-milling).

The tool path factor does not affect the geometrical responses variability, at least at high nominal wall thickness while Figure 7 points out as, for a low wall thickness, wall deformation is more severe when machining with Waterline tool path and down-milling strategy. The tool path could perhaps influence the wall texture, but, if some marks exist on the finished

walls, they are not seen by mean thickness measurements, because the 1 mm CMM probe tip radius acts as a mechanical filter covering this small scale geometrical errors.

Summarizing the aforementioned results, in order to achieve the best accuracy in thin walls micromilling operations, it is suggested to apply Step Support tool path and Up-milling strategy.

4.2. Relationship between nominal workpiece characteristics / process parameters and cutting forces

A three factors (Thickness, Strategy and Tool path) complete model plus the covariate ΔR_{cum} (cumulative tool radius variation) has been analyzed also to study the relationship between the nominal workpiece characteristics / process parameters and the cutting forces (“2”, red arrow in Figure 1).

The results of ANCOVA on force coefficients are presented in Table 3 while Figure 15, 16 and 17 depict the results related to force coefficients for each factor.

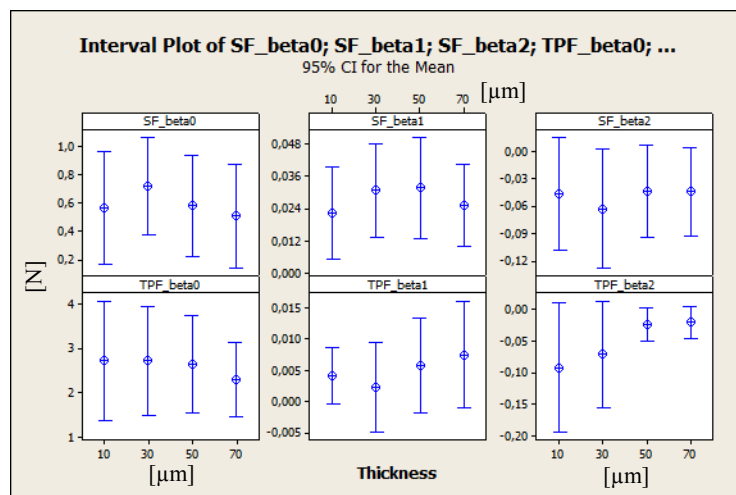


Figure 15. Interval value plots of force coefficients against Thickness factor.

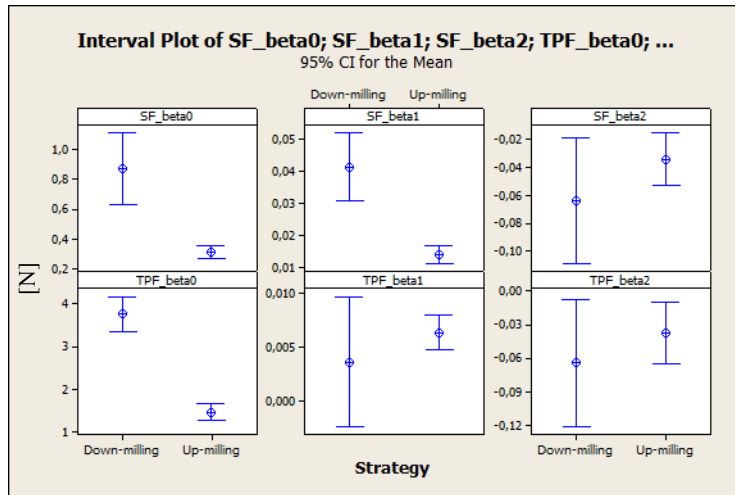


Figure 16. Interval value plots of force coefficients against Strategy factor.

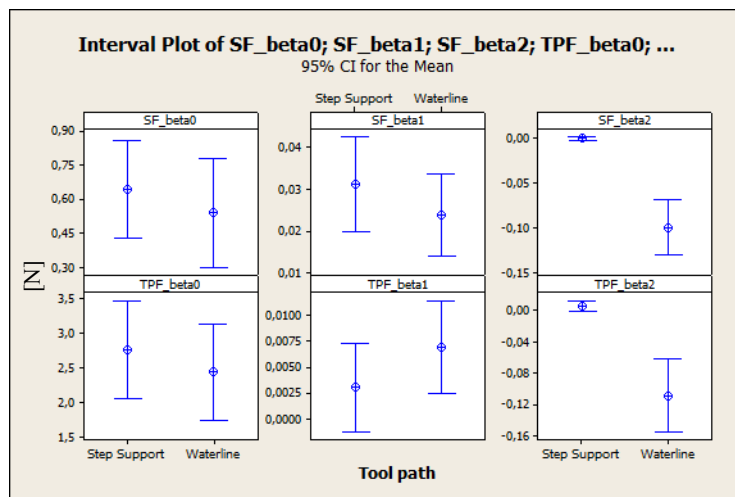


Figure 17. Interval value plots of force coefficients against Tool path factor.

The covariate (i.e. the cumulative tool radius variation) has an influence on nearly all the cutting force coefficients; this demonstrates how the covariate use has been effective in removing the nuisance effect of tool wear also in this case.

As concerning the nominal wall thickness, it affects only the oscillation amplitude β_2 of TPF (Table 3). As the wall thickness decreases, its stiffness reduces and its deflection under cutting forces increases; therefore forces vary when

machining opposite wall sides. Figure 15 shows how TPF β_2 absolute value (the sign should not be taken into account since it just arises from the model in Eq. 2) is maximum at the lowest wall thickness. It can be noticed that SF β_2 and TPF β_2 upper limit is always nearly zero since it accounts for tests performed with the Step Support strategy, which avoids the wall bending even at low wall thickness.

As regarding the milling strategy, the ANCOVA results point out how it is significant on all the coefficients β_0 , β_1 and β_2 for SF and β_0 and β_2 coefficients for TPF (Table 3). The strategy plays a role on force coefficients since the F_x absolute value is higher in Down-milling than in Up-milling, as it can be noticed in Figure 16.

The tool path has an influence on the oscillation amplitude β_2 of both SF and TPF (Table 3). When milling with the Waterline tool path, the thin wall bending is higher for even steps (Figure 3), therefore the radial depth of cut, the maximum uncut chip thickness and the consequent cutting forces vary more than in case of milling with the Step Support tool path (see Figure 17). SF β_2 and TPF β_2 are close to zero in this latter case since wall is always well supported and forces do not sensibly vary along the steps.

These results allow to define some preliminary criteria to choose the correct parameters combination for obtaining the desired cutting forces in case of thin wall micromilling. For example, if the target is to reduce the cutting force oscillation when milling opposite wall sides, a higher wall thickness and/or the Step Support tool path should be preferred. Moreover, a low absolute cutting force value can be achieved by using Up-milling strategy instead of Down-milling.

4.3 Relationship between cutting forces and workpiece quality

A linear regression analysis has been performed to study the relationship between the workpiece geometrical quality and the cutting forces (“3”, red arrow in Figure 1).

A correlation test (Table 4) showed that SF β_1 , TPF β_0 and TPF β_1 are correlated to SF β_0 (first column of Table 4) while TPF β_2 is correlated to SF β_2 ; therefore, only SF β_0 and SF β_2 have been included in the regression model to avoid collinearity problems.

Table 4. Correlation coefficients and p-values in brackets (dark grey = significant correlation, grey = nearly significant correlation).

| | SF β_0 | SF β_1 | SF β_2 | TPF β_0 | TPF β_1 |
|---------------|--------------------|--------------------|--------------------|--------------------|--------------------|
| SF β_1 | 0.947 (0.000) | | | | |
| SF β_2 | - 0.342 (0.056) | -0.205 (0.261) | | | |
| TPF β_0 | 0.743 (0.000) | 0.804 (0.000) | - 0.207 (0.255) | | |
| TPF β_1 | - 0.689 (0.000) | - 0.597 (0.000) | 0.051 (0.783) | - 0.218 (0.230) | |
| TPF β_2 | - 0.071 (0.699) | 0.006 (0.974) | 0.732 (0.000) | - 0.180 (0.323) | - 0.216 (0.234) |

The regression analysis shows how SF β_0 and SF β_2 influence both the average thickness error and the total flatness deviation, hence all the cutting force coefficients which are correlated to SF β_0 and SF β_2 have an effect on the workpiece quality responses as well. The main results (p-values) of the regression analysis have been summarized in Table 5 while the estimated regression models (coded predictors) of the two responses are the following (terms in square brackets refer to nearly significant factors).

$$err = [-0.035 \cdot SF\beta_0 - 0.0491 \cdot SF\beta_2 + 0.385 \cdot (SF\beta_0 \cdot SF\beta_2)] + 0.02741 \cdot (SF\beta_0)^2 + 0.0689 \cdot (SF\beta_2)^2 \quad \sigma = 0.0164 \quad (3)$$

$$flatness_dev = [-0.0594 \cdot SF\beta_0 - 0.0628 \cdot SF\beta_2] + 0.0773 \cdot (SF\beta_0 \cdot SF\beta_2) + 0.0515 \cdot (SF\beta_0)^2 [+0.0843 \cdot (SF\beta_2)^2] \quad \sigma = 0.2195 \quad (4)$$

Table 5. Regression analysis p-values (dark grey = significant factor, grey = nearly significant factor, $\alpha = 1\%$).

| | | | | |
|--------------|--------------|-----------------------------|----------------|----------------|
| SF β_0 | SF β_2 | SF β_0 * SF β_2 | SF β_0^2 | SF β_2^2 |
|--------------|--------------|-----------------------------|----------------|----------------|

| | | | | | | |
|---------------|--------------------|-------|-------|--------------|--------------|--------------|
| Wall geometry | Thickness error | 0.052 | 0.061 | 0.071 | 0.006 | 0.009 |
| | Flatness deviation | 0.016 | 0.037 | 0.009 | 0.000 | 0.015 |

5. CONCLUSIONS AND FUTURE DEVELOPMENTS

The present paper has investigated the effect of some nominal workpiece characteristics / process parameters (wall thickness, milling strategy and tool path) on wall quality (thickness error and flatness deviation) and cutting forces (six coefficients describing the profile of SF and TPF harmonic components along milling steps) in high aspect ratio walls micromilling. Moreover, it has quantitatively studied the relationship between cutting forces and workpiece geometrical quality in order to prove the feasibility of a general approach able to meet tolerances by controlling forces. A suitable experimental campaign has been designed and the tool wear effect has been statistically removed by considering the cumulative tool radius variation as covariate.

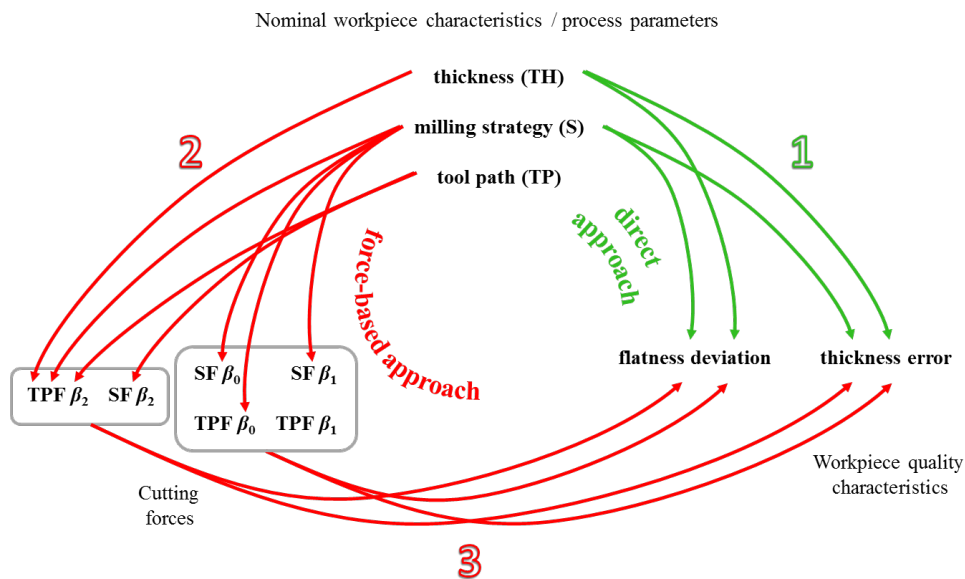


Figure 18. Summary of paper findings.

The arrows in Figure 18 summarize all the found relationships (Section 4.1, 4.2 and 4.3). The presented results concerning the direct approach for workpiece quality prediction (“1”, green arrows in Figure 18) can be used to choose the correct parameters combination for producing the desired wall quality and thus allow to improve the current thin wall micromilling accuracy. On the other hand, the results related to the force-based approach (“2” and “3”, red arrows in Figure 18) allow to know the suitable cutting force coefficients to have the desired cutting forces and then to choose the suitable parameters combination for obtaining these cutting force coefficients. Hence, the force-based approach seems to be more powerful than the direct approach because both allow to select the correct process parameters, but the force-based approach takes into account physical quantities, such as cutting forces, that can be used for process monitoring and controlling purposes.

ACKNOWLEDGMENTS

The authors are very grateful to the “MI_crolab” staff, in particular Francesco Cacciatore and Eligio Grossi, for their invaluable support to the presented research.

This study has been partly founded by Regione Lombardia, within the project “REMS: Rete Lombarda di Eccellenza per la Meccanica Strumentale e Laboratorio Esteso / Excellence Network for Instrumental Mechanics and Extended Laboratory” (Fondo per la promozione di Accordi istituzionali, d.reg. n°4779 del 14/5/2009), and by the European Union Seventh Framework Programme FP7/2007-2013, under grant agreement n° 285075 (MuProD).

REFERENCES

- [1] Dornfeld, D., Min, S., Takeuchi, Y., 2006,. Recent advances in mechanical micromachining, *CIRP Annals - Manufacturing Technology*, 5: 745-768.
- [2] Masuzawa, T., 2000, State of the art of micromachining, *CIRP Annals - Manufacturing Technology*, 49: 473-488.
- [3] Tosello, G., Bissacco, G. Tang, P.T., Hansen, H.N., Nielsen, P.C., 2008, High aspect ratio micro tool manufacturing for polymer replication using μ EDM of silicon, selective etching and electroforming, *Microsystem technologies*, 14:1757–1764.
- [4] Annoni, M., Petrò, S., Rebaioli, L., Semeraro, Q., Solito, R., 2012, Micromilling strategies impact on thin walls geometrical quality, *4M 2012 - 9th International Conference on Multi-Material Micro Manufacture*, Wien (Austria).
- [5] Li, P., Zdebski, D., Langen, H.H., Hoogstrate, A.M., Oosterling, J.A.J., Schmidt, R.H.M., Allen, D.M., 2010,

Micromilling of thin ribs with high aspect ratios, *Journal of Micromechanics and Microengineering*, 20.

- [6] Popov, K., Dimov, S., Pham, D.T., Ivanov, A., 2006, Micromilling strategies for machining thin features, *Proceedings of the Institution of Mechanical Engineers, Part C: Journal of Mechanical Engineering Science*, 220: 1677-1684.
- [7] Llanos, I., Agirre, A., Urreta, H., Thepsonthi, T., Özel, T., 2014, Micromilling high aspect ratio features using tungsten carbide tools, *Proceedings of the Institution of Mechanical Engineers, Part B: Journal of Engineering Manufacture*.
- [8] K.M.Y. Law, A. Geddam, Error compensation in the end milling of pockets: a methodology, *Journal of Materials Processing Technology* 139 (2003) 21–27.
- [9] S. Ratchev, S. Liu, W. Huang, A.A. Becker, A flexible force model for end milling of low-rigidity parts, *Proceedings of AMPT, Dublin, 2003* pp. 836–839.
- [10] S. Ratchev, W. Huang, S. Liu, A.A. Becker, Modelling and simulation environment for machining of low rigidity components, *Proceedings of AMPT, Dublin, 2003* pp. 313–316.
- [11] S. Ratchev, S. Liu, W. Huang, A.A. Becker, A flexible force model for end milling of low-rigidity parts, *Journal of Materials Processing Technology* 153/154 (2004) 134–138.
- [12] S. Ratchev, W. Huang, S. Liu, A.A. Becker, Modelling and simulation environment for machining of low-rigidity components, *Journal of Materials Processing Technology* 153/154 (2004) 67–73.
- [13] S. Ratchev, S. Liu, W. Huang, A.A. Becker, Milling error prediction and compensation in machining of low-rigidity parts, *International Journal of Machine Tools and Manufacture* 44 (2004) 1629–1641.
- [14] Wan M, Zhang WH, Qin GH, Wang ZP (2008) Strategies for error prediction and error control in peripheral milling of thin-walled workpiece. *International Journal of Machine Tools and Manufacture* 48 : 1366-1374.
- [15] Annoni, M., Petrò, S., Rebaioli, L., Semeraro, Q., Solito, R., 2012, Process parameters effect on cutting forces and geometrical quality in thin wall micromilling, *NAMRC 41 – 41st North American Manufacturing Research Conference, Madison (USA)*.
- [16] R. Ramesh, M.A. Mannan, A.N. Poo, Error compensation in machine tools—a review. Part I: geometric, cutting-force induced and fixture dependent errors, *International Journal of Machine Tools and Manufacture* 40 (2000) 1235–1256.
- [17] R. Ramesh, M.A. Mannan, A.N. Poo, Error compensation in machine tools—a review. Part II: thermal errors, *International Journal of Machine Tools and Manufacture* 40 (2000) 1257–1284.

- [18] S.M. Wang, Y.L. Liu, Y. Kang, An efficient error compensation system for CNC multi-axis machines, *Int. J. Mach. Tools Manufact.* 42 (2002) 1235–1245.
- [19] D. Gao, Y.X. Yao, W.M. Chiu, F.W. Lam, Accuracy enhancement of a small overhung boring bar servo system by real-time error compensation, *Precision Engineering* 26 (2002) 456–459.[20] Chen W, Xue J, Tang D, Chen H, Qu S (2009) Deformation prediction and error compensation in multilayer milling processes for thin-walled parts. *International Journal of Machine Tools and Manufacture*, 49 : 859-864.[21] Friedrich, C.R., Vasile, M.J., 1996, Development of the micromilling process for high-aspect-ratio microstructures, *Journal of Microelectromechanical Systems*, 5: 33-38.
- [22] Bang, Y.B., Lee, K.M., Oh, S., 2005, 5-axis micro milling machine for machining micro parts, *International Journal of Advanced Manufacturing Technology*, 25: 888–894.
- [23] T. Gietzelt, L. Eichorn, K. Schubert, Manufacturing of microstructures with high aspect ratio by micromachining, *Microsystem Technologies*, 14 (2008) 1525-1529.
- [24] Y. Okazaki, T. Mori, N. Morita, Desk-top NC milling machine with 200 krpm spindle, *Proceedings of the ASPE*, 2001.
- [25] Y. Okazaki, Desk-top ultra-high-speed milling machine with 300krpm spindle and linear motor stages, *Proceedings of the ASPE*, 2004.
- [26] ISO 3002-1: 1982, Basic quantities in cutting and grinding - Part 1: Geometry of the active part of cutting tools - general terms, reference systems, tool and working angles, chip breakers.
- [27] ISO 3002-3: 1984, Basic quantities in cutting and grinding - Part 3: geometric and kinematic quantities in cutting.
- [28] Solito, R., 2011, *Microfresatura di pareti sottili / Thin walls micromilling*, Master thesis, Politecnico di Milano.
- [29] ISO 10360-5: 2010, Geometrical product specifications (GPS) – acceptance and reverification tests for coordinate measuring machines (CMM) – part 5: CMMs using single and multiple stylus contacting probing systems.
- [30] ISO 14405-1: Geometrical product specifications (GPS) - Dimensional tolerancing - Part 1: Linear sizes, 2010.
- [31] Anthony, G.T., Anthony, H.M., Bittner, B., Butler, B.P., Cox, M.G., Drieschner, R., Elligsen, R., Forbes, A.B., Gross, H., Hannaby, S.A., Harris, P.M., Kok, J., 1996, Reference software for finding Chebyshev best-fit geometric elements, *Journal of the International Societies for Precision Engineering and Nanotechnology*, 19: 28 – 36.